

RESEARCH

Open Access



# A single-cell transcriptomic atlas of human lens epithelium: identification and functional insights into lens stem/progenitor cells

Yuzhou Gu<sup>1†</sup>, Lu Chen<sup>1†</sup>, Shuying Chen<sup>1</sup>, Yuhao Wu<sup>1</sup>, Shengjie Hao<sup>1</sup>, Feiyin Sheng<sup>1</sup>, Jiali Yuan<sup>1,2</sup>, Zhenwei Qin<sup>1</sup>, Di Wu<sup>1</sup>, Yu Han<sup>1</sup>, Zengying Yao<sup>1</sup>, Zhijian Chen<sup>3</sup>, I. Michael Wormstone<sup>2</sup>, Yibo Yu<sup>1\*</sup>, Junbin Qian<sup>1,4\*</sup>, Qiuli Fu<sup>1\*</sup> and Ke Yao<sup>1\*</sup> 

## Abstract

**Background** The existence of stem/progenitor cells in the lens epithelium has been demonstrated, but their identification remains challenging. Accurate identification requires advanced technologies and a comprehensive understanding of lens epithelial cell (LEC) subtypes, presenting a significant challenge in age-related cataract research.

**Methods** Eight pairs of human donor lens epithelium samples were collected for single-cell RNA sequencing (scRNA-seq). This included four non-aged (< 65 years) and four aged (> 65 years) individuals. Subsequent analyses involved cell (sub)type characterization, trajectory inference, and cell–cell communication. Experimental validation was conducted through transcriptome sequencing and immunofluorescence on human lenses, lens organoids, rabbit regenerated lenses, mouse lenses, and cell lines.

**Results** Six groups were identified via UMAP mapping of scRNA-seq data: four LECs, one lens fiber cells (LFCs), and one immune cells. One of the four LEC clusters exhibited a distinct gene expression profile and was identified as transient amplifying cells (TACs). TACs specifically express TOP2A and are localized at the lens equator. CytoTRACE analysis to the LEC and LFC data sets provided a differentiation trajectory. The TAC group was determined as stage 2 in the trajectory and LFCs last. The 3 sub groups were labelled early, mid and late LECs and corresponded to stage 1, 3 and 4 in the path. While cell population demographics remained stable with age, transcriptomic changes in LECs were observed, including weaker intercellular crosstalk and adhesion, and fewer TACs in S phase. Lens progenitor-like cells (LPLCs) were identified as a sub-population in early LECs and express ID1. In addition, pleiotrophin (PTN) signaling was prevalent at all differentiation stages, with a notable weakening of PTN signaling in aged LPLCs.

**Conclusions** This study identified four subclasses of LECs within the human lens epithelium that follow a progressive staged development pathway from progenitor cells to mature LECs. TOP2A can serve as a biomarker for TAC

<sup>†</sup>Yuzhou Gu and Lu Chen been contributed equally to this work.

\*Correspondence:

Yibo Yu

yuyibo@zju.edu.cn

Junbin Qian

dr\_qian@zju.edu.cn

Qiuli Fu

2313009@zju.edu.cn

Ke Yao

xlren@zju.edu.cn

Full list of author information is available at the end of the article



in the lens, and LPLCs sustain their dedifferentiated state by expressing ID1. The aging process does not appear to alter cell population demographics, but significant alteration in gene expression profile is observed. Moreover, PTN signaling emerges as a crucial factor in lens homeostasis and represents a potential target for cataract drug development.

**Keywords** scRNA-seq, Aging, Lens epithelial cell, Transient amplifying cell, Lens stem cell

## Background

Cataracts remain the leading cause of blindness worldwide, with age-related cataracts (ARCs) being the most prevalent type, affecting approximately 80% of individuals aged 60 to 89 [1–3]. Lens epithelial cells (LECs) play a critical role in maintaining lens transparency and physiological function [4]. It has been established that LEC dysfunction disrupts lens homeostasis with aging, contributing to the development of ARCs [4, 5]. Therefore, LECs have long been a central focus of cataract pathogenesis research and drug development.

It is well established that the equatorial region of the lens epithelium serves as the site for cell division and differentiation of LECs into lens fiber cells (LFCs) [4, 5]. The central region of the epithelium is generally considered a non-dividing cell population. Although mitotic activity is limited, these cells remain functionally active and are essential for lens maintenance and homeostasis. Cells within the epithelium, particularly in the central region, comprise a large population of truly aged cells that have persisted since embryonic development [5, 6]. This population of cells therefore provides insights not only into the effects of aging in the lens but also into cellular aging itself. Functional clustering analysis revealed age-related differences, with genes regulating translation, protein synthesis, stress responses, and cell transport being upregulated, while genes involved in repair systems and matrix regulation were downregulated [7, 8]. In other organs and tissues, such as the skin, intestines, and cornea, the decline in self-renewal of adult stem cells with age leads to tissue senescence [9]. This suggests that the lens epithelium may also rely on adult stem/progenitor cells to maintain homeostasis and counteract aging-related factors.

The presence of stem/progenitor cells in the lens epithelium has been supported by numerous studies [10–13]. Adult stem cells exhibit robust tissue repair capacity and are both morphologically and functionally primitive. However, the identification of these stem cells remains challenging. Previous attempts have relied on two main approaches, one of which involves labeling infrequent or slow-cycling stem cells with DNA precursors such as tritiated thymidine (3H-TdR). Although 3H-TdR labeling has demonstrated a high proportion of labeled LECs,

this does not accurately reflect adult stem cells [12]. The second approach is based on specific markers. The use of classical adult stem cell markers, such as SOX2, MSIL, and LGR4, has also proven unreliable for the specific identification of lens stem cells using conventional immunohistochemistry [11, 14]. Thus, accurate identification of lens stem/progenitor cells requires advanced technologies and a comprehensive understanding of LEC subtypes, posing a significant challenge in cataract basic research.

Single-cell RNA sequencing (scRNA-seq) has advanced rapidly in recent years, providing high-resolution insights into cellular heterogeneity and enabling the identification of transient amplifying cells (TACs) and adult stem cells in other tissues [15–17]. In this study, we utilized scRNA-seq to analyze human lens epithelium samples, enabling the transcriptomic identification of subpopulations within the lens epithelium at single-cell resolution. This approach identified six cell populations within the lens epithelium, including TACs and lens progenitor-like cells (LPLCs). Trajectory analysis revealed a sequential progression from lens progenitor cells to mature epithelial cells. The overall cell population demographics did not differ significantly with age, but significant changes in gene expression profiles were observed.

## Materials and methods

### Human lens samples and cell isolation

Eyes from 9 organ donors were obtained from the Eye Bank of the Second Affiliated Hospital of Zhejiang University. The study was approved by the Human Ethics Committee of the Second Affiliated Hospital of Zhejiang University School of Medicine and adhered to the Declaration of Helsinki. For this study, 16 lenses were categorized into aged and non-aged groups, using 65 years as the cutoff for aged group, in accordance with the World Health Organization's definition. Details on donor screening criteria and donor information are provided in Text S1.

Within 6 h of death, both eyes were removed from each donor. After eye bank staff cut off the corneas for transplantation, the lenses were detached, cleaned of attached tissues (e.g., iris, suspensory ligaments), and photographed under a stereomicroscope. The lenses were then

immersed in saline for single-cell suspension preparation (8 samples in total, each consisting of 2 lenses from the same donor) and flat-mounted lens capsule immunofluorescence (2 lenses from the same donor, 64 years old, female). All procedures were completed within 2 h post-eye removal.

For the 16 lenses, an incision was made to separate the anterior capsule from the posterior capsule, starting from the equatorial part of the lens, about one-fourth the length of the equatorial circumference. The anterior capsule was peeled away from the lens fibrous tissue, followed by the posterior capsule. Larger capsule fragments were cut with microscopic scissors. Capsule fragments from 2 lenses of the same donor were immersed in 1 mL of digestion solution (0.25% trypsin and 0.02% EDTA, Gibco, USA) and incubated at 37 °C for 3 min. Digestion was terminated with 2 mL of DMEM/F12 medium (Corning, USA) containing 5% fetal bovine serum (FBS, AusGeneX, Australia). The sample was pipetted gently to disperse cell clusters into individual cells. After filtering through a 40 µm pore size filter, the sample was centrifuged at 300xg for 4 min. The supernatant was discarded, and cells were resuspended in 50 µL of PBS with 0.04% BSA as a single-cell suspension (200–700 live cells/µL). The samples were used promptly for scRNA-seq.

#### scRNA-seq and data analysis

scRNA-seq libraries were prepared using the Chromium Single Cell 3' Library Preparation Kits and Gel Bead & Multiplex Kits from 10×Genomics. Our goal was to profile a total of 5000 cells per library, provided that an adequate number of cells were preserved throughout the dissociation process. Sequencing was performed on the MGISEQ2000 platforms. The minimum sequencing saturation is not less than 40.5%. The generated scRNA-seq data were merged and analyzed using R (version 4.2.3) and the Seurat R package (version 5.0.3). In the preliminary phase, post-Cell Ranger's metric evaluation, cells exhibiting less than 200 or more than 5000 gene detections and a mitochondrial gene proportion exceeding 20% were omitted from further analytical processes. Specifically, cells with a high percentage of hemoglobin-related genes (`percent_hb`) or ribosomal genes (`percent_ribo`) were filtered out. Thresholds were empirically determined based on the distribution of each metric across all cells. Cells were retained for further analysis only if they exhibited `percent_hb` value below 20% and `percent_ribo` value below 20%. These thresholds ensured the removal of stressed or dying cells, as well as cells with high ambient RNA contamination. Upon the above stringent quality control measures, a dataset comprising 56,717 cells was retained for subsequent computational analyses. Dimensionality reduction was carried out and

visualized through Uniform Manifold Approximation and Projection (UMAP). Cluster annotation was conducted using marker genes derived from established literature and by analyzing gene expression patterns across clusters within our dataset. Gene Ontology (GO) analysis of differentially expressed genes (DEGs), trajectory analysis and cell–cell communication analysis were conducted using the CytoTRACE R package (version 0.3.3), Velocyto pipeline, and CellChat R package (version 1.6.1). Detailed methodologies are described in Text S2.

#### Lens organoid

H9 human embryonic stem cells (ESCs, WiCell Research Institute, Inc., USA) were cultured in mTesR medium (Stemcell, Canada) on Matrigel-coated six-well dishes (Corning, USA) and differentiated into lens organoids using the “fried egg” method, as detailed in previous studies [18–20]. In brief, the ESCs were induced to differentiate into the ectoderm/neuroectoderm via noggin until epithelial-like cells first appeared on day 6. FGF and BMP signaling were then activated through bFGF, BMP4, and BMP7. Cell clusters with a “fried egg” structure were observed on day 11. On day 15, BMP4 and BMP7 were replaced with WNT3A to trigger the differentiation of LECs into LFCs. By day 23 of culture, mature lens organoids, which are transparent, refractive, and exhibit lens-like structural and molecular characteristics, were obtained. This *in vitro* system effectively emulates cell growth and differentiation in human lens. To perform transcriptome sequencing on lens organoids at different developmental stages, total RNA was extracted (sampled at day 0, 3, 4, 5, 6, 10, 15 and 23) using TRIzol Reagent (Invitrogen, USA). Three biological replicates were prepared. Details on transcriptome sequencing methods are provided in Text S5.

#### Quantitative real-time PCR

TRIzol Reagent (Invitrogen, USA) was used to obtain total RNA from lens organoids during 23-days culture period (sampled at day 0, 5, 10, 15 and 23, 3 repetitions for each group) and the cDNA was synthesized using PrimeScript™ RT Master Mix (Takara, China). With an ABI Fast 7500 RT-PCR system (Life Technologies, v2.0.6), quantitative real-time PCR (qRT-PCR) was carried out using SYBR Premix Ex Tag™ (Takara, China). Internal control was Glyceraldehyde-3-phosphate dehydrogenase (GAPDH). Table S1 in the Supplementary Materials lists all primers.

#### HLECs scratch model

The human lens epithelial cells (HLECs, SRA01/04) scratch model was employed to simulate the lens

epithelium damage repair process. Since the scratches were largely healed after 24 h, immunofluorescence staining was performed at 6, 12, and 24 h post-scratching. Details of the scratch model procedures are outlined in Text S3.

### Rabbit lens regeneration model

A novel method for constructing a rabbit lens regeneration model has been described in our recent publication [21]. The experiments are in strict accordance with ethical approval. Prior to surgery, surgical-depth anesthesia was induced by intravenous administration of sodium pentobarbital in saline (3 mg/100 mL). Euthanasia was carried out by intravenous injection of an overdose of sodium pentobarbital (150 mg/kg). Sodium pentobarbital (Sigma-Aldrich, USA) was prepared in sterile saline at a concentration of 60 mg/mL. The solution was administered slowly into the marginal ear vein. Death was confirmed by the absence of a heartbeat and cessation of breathing. This model reflects the *in vivo* process of lens epithelial damage repair. The regenerated lenses at 2 and 4 weeks post-surgery were dissected to prepare flat-mounted lens capsules and frozen sections for immunofluorescence staining. Experimental and surgical details are provided in Text S4.

### Immunofluorescence

Lens organoids at various differentiation stages, flat-mounted lens capsules from humans and rabbits, frozen sections of rabbit regenerated lenses, and scratched HLECs were fixed with 4% paraformaldehyde in PBS, permeabilized with 0.5% Triton X-100 (Sigma-Aldrich, USA) in PBS for 25 min, and incubated overnight at 4 °C with primary antibodies (TOP2A polyclonal antibody, 1:25, Proteintech, China; ID1 polyclonal antibody, 1:50, Proteintech, China). Following this, samples were incubated with secondary antibodies (Anti-rabbit IgG, 1:1000, Cell Signaling Technology, USA). Nuclei were labeled with 1 µg/mL of 4,6-diamido-2-phenylindole dihydrochloride (DAPI, Sigma-Aldrich, USA). Images were captured using a Zeiss LSM 900 confocal microscope (Carl Zeiss AG, Germany).

### Mice and transcriptome sequencing

Total RNA was extracted from mice lenses using TRIzol Reagent (Invitrogen, USA). Three biological replicates were prepared. The experiments are in strict accordance with ethical approval. Anesthesia was not administered as the experimental procedures did not involve invasive interventions. Euthanasia was performed by intravenous injection of an overdose of sodium pentobarbital (150 mg/kg). Sodium pentobarbital (Sigma-Aldrich, USA) was dissolved in sterile saline to achieve

a concentration of 60 mg/mL. The solution was administered via the tail vein. Death was confirmed by the absence of a heartbeat and cessation of breathing. Details on mouse husbandry, experimental procedures, and transcriptome sequencing methods are provided in Text S5.

### Statistical analysis

Data are presented as the mean ± SD. Statistical analyses were performed using GraphPad Prism 8.0 (GraphPad Software, USA) with unpaired Student's t-test. P values lower than 0.05 are considered statistically significant.

## Results

### Identification of human lens epithelium cell types using scRNA-seq

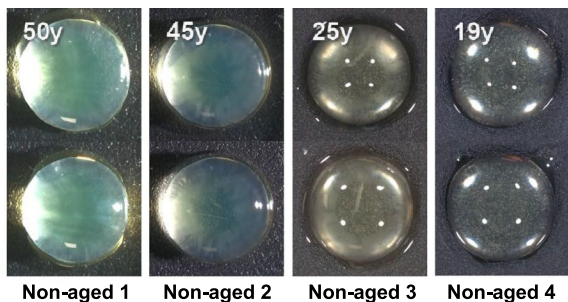
Human lenses from four non-aged individuals (19, 25, 45, and 50 years) and four aged individuals (70, 71, 72, and 73 years) were used in the study. Increased brunescence was prominent in lenses obtained from aged donors (Fig. 1A), providing evidence of biological aging. One of the lenses in Aged 3 (71 years) had a clearly observable cataract (Area of red dotted lines), the others did not meet diagnostic criteria. Lens epithelium from each donor was processed to generate single-cell suspensions for scRNA-seq and subsequent analysis (Fig. 1B). Cells that failed quality control tests were filtered from the study. In total, transcriptome profiles of 56,717 individual cells were obtained.

To determine whether the population was homogeneous or exhibited diversity, UMAP was employed. This approach identified six distinct clusters within the overall population of isolated cells (Fig. 2A–C). The clusters were classified as LFCs, early-differentiating lens epithelial cells (eLECs), mid-differentiating lens epithelial cells (mLECs), late-differentiating lens epithelial cells (ILECs), TACs, and immune cells (ICs). The abundance of each group varied, with the majority of cells classified as mLECs and ILECs (Fig. 2B and C). The cell classification/labeling of each cluster resulted from the following approaches and subsequent findings.

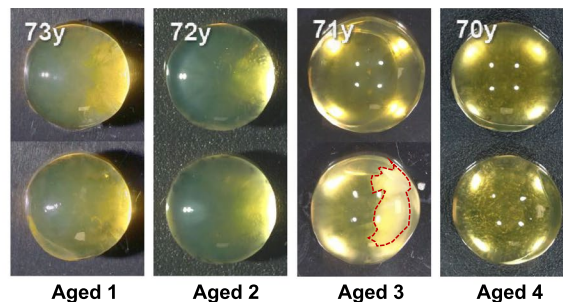
Having determined six clusters, further analysis evaluated the expression profiles of marker genes for cells likely present in the isolated population (Fig. 2D and E). Genes including *PAX6* and *AQP1* were used as markers for the lens epithelial cell population. Four clusters demonstrated high expression of both these markers indicating that they were all isolated lens epithelial cells. *CRYBA1* and *CRYBB1* were abundant in one cluster, which strongly indicates a small population of lens fiber cells were present. Distinct expression of immune cell markers, including *PTPRC*, were also evident in a single cluster.

**A**

**Lenses from non-aged donors**



**Lenses from aged donors**



**B**

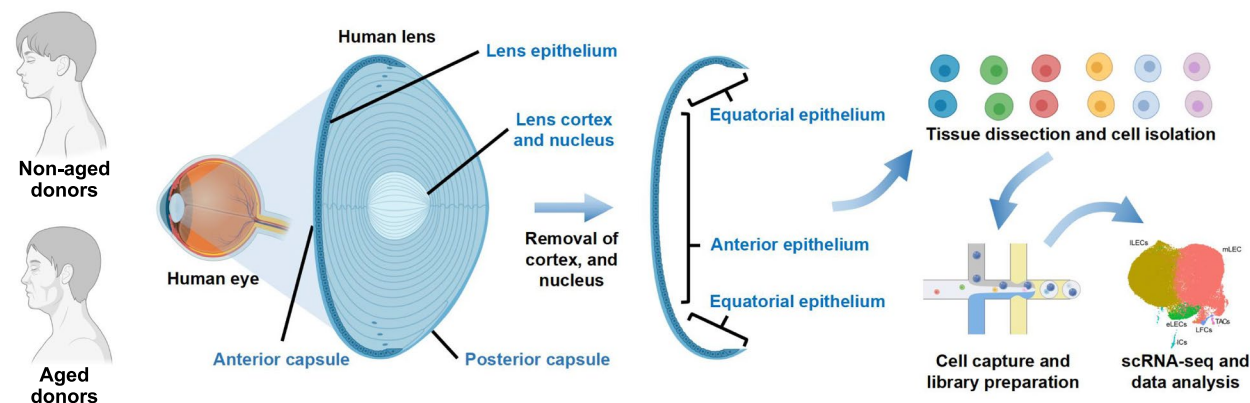


**Fig. 1** scRNA-seq analysis of human lens of different ages. **A** Eight pairs of donated human lenses for scRNA-seq were divided into non-aged (<65 years) and aged (≥65 years) groups. Red dashed lines indicate cataract-affected regions observed in the lenses. **B** Schematic diagram of the lens epithelium anatomical structure and scRNA-seq sample preparation

(See figure on next page.)

**Fig. 2** Identification of human lens epithelium cell types using scRNA-seq. **A** Heatmap of cell-type-specific gene signatures. Columns represent clustered cell types, rows show expression of genes. Color scale indicates relative expression levels. **B** UMAP visualization of 56,717 single-cell transcriptomes colored by annotated cell types. **C** Cellular composition analysis. Bar heights indicate relative abundance of each cell type (percentage of total cells), with absolute cell counts labeled. Epithelial subtypes dominate. **D** Dot plot of marker genes across cell types. Dot size represents percentage of cells expressing the gene; color intensity shows mean normalized expression. **E** Spatial expression patterns of representative markers projected onto UMAP coordinates. The color key from gray to purple indicates low to high gene expression levels. Solid boxes: definitive cell-type markers; dashed boxes: genes with relative enrichment in specific cell types

The identified cell types and their relative abundances align with expectations. Therefore, it was necessary to understand the differences between the four LEC clusters and determine their putative roles within the lens. The gene expression patterns for each cluster provide a motif that is indicative of their role or function within the epithelium. The cluster identified as TACs exhibits clear markers of cell division, such as *TOP2A*, suggesting that it represents a distinct population of proliferating LECs (Fig. 2D and E). However, the number of TACs was notably low, with only 96 cells identified

in eight pairs of lenses (Fig. 2C), consistent with the well-documented low rate of cell division in the lens epithelium. The other three clusters of LECs have no specific markers, but each have their own motif of relatively higher expressed genes, such that eLECs had high expression of *TMEM256*, *DDT*, and *SCGB1D2*, mLECs expressed *DACH2*, *OPCML*, and *PLCXD3*, and lLECs showed relatively high expression of *SFRP1*, *ATP8B4*, and *GRIA4* (Fig. 2D and E). These expression profiles provide insights into specific roles within the lens epithelium; however, to fully utilize the data, CytoTRACE

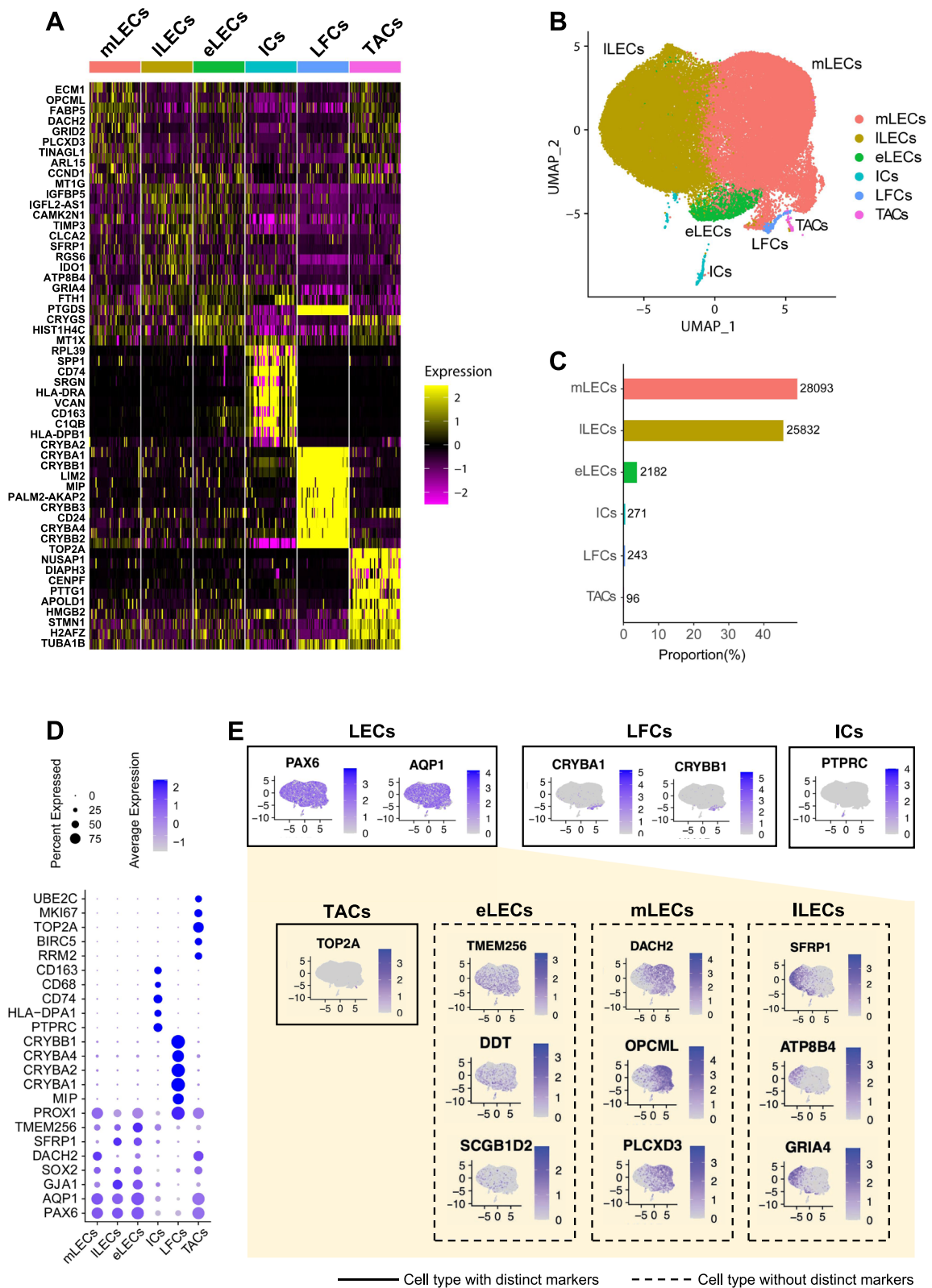


**Fig. 2** (See legend on previous page.)

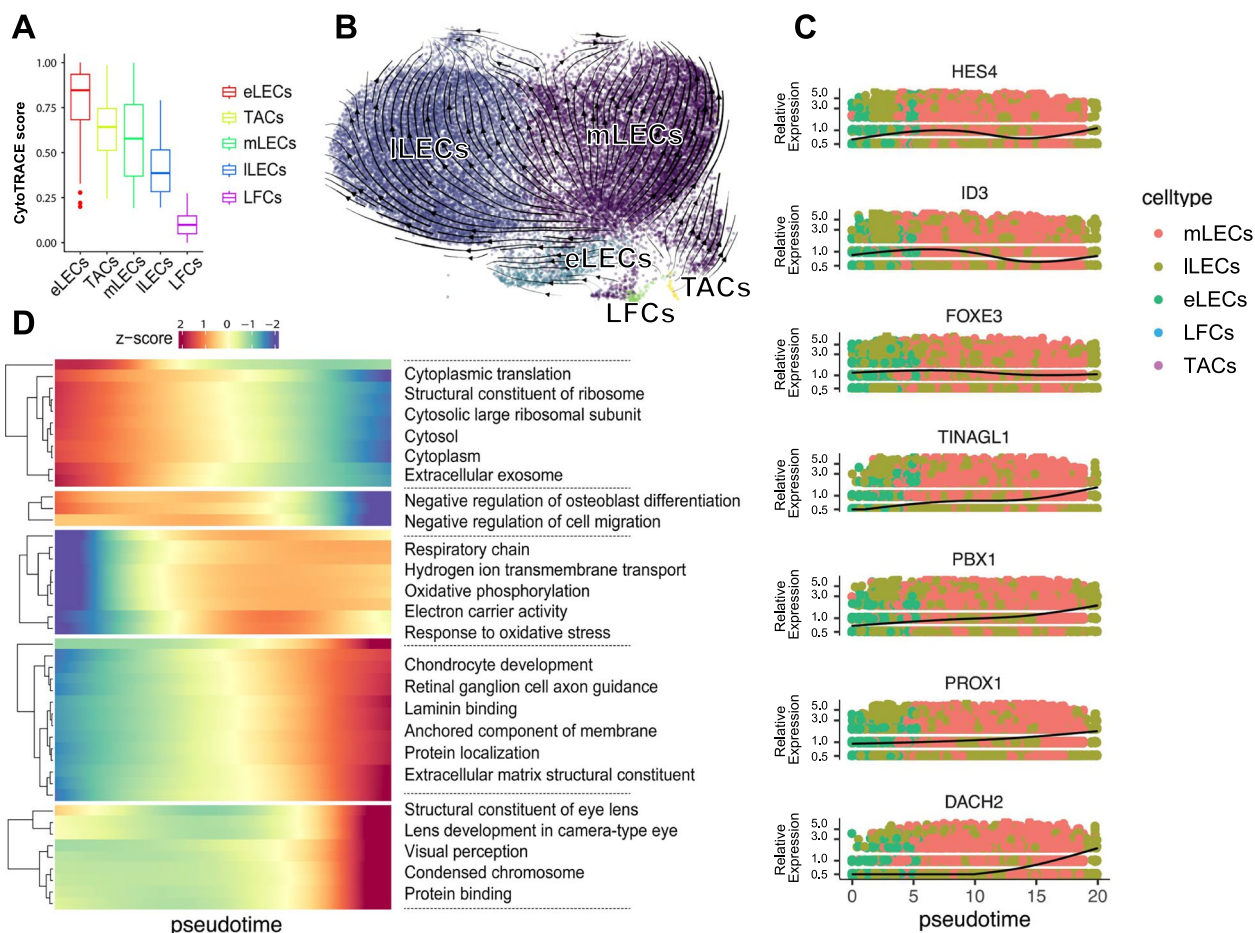


**Fig. 3** Reconstructing the Developmental Pseudotime Trajectory of lens epithelium. **A** CytoTRACE analysis of differentiation potential across cell clusters, with higher scores indicating greater developmental potential. **B** RNA velocity projection embedded in UMAP space. Projection of the velocity field arrows onto the UMAP plot depicted the order of differentiation. **C** Representative epithelial-differentiation-related gene expression dynamics along differentiation trajectory. **D** Heatmap showing the gene expression dynamics along differentiation trajectories, the color key from blue to red indicates low to high gene expression levels. Top gene ontology annotations of indicated biological process among each timepoint are listed to the right

analysis of differentiation trajectories was performed. This indicated a progressive pathway of lens maturation across five clusters (recognized as LECs or LFCs) (Fig. 3A). Projection of the velocity field arrows onto the UMAP plot depicted the general trend of differentiation (Fig. 3B). TACs and LFCs represent distinct components within this pathway. TACs were identified as the second stage, while LFCs, as expected, represented the fifth and final stage (Fig. 3A). The three remaining clusters were located at stages 1, 3 and 4 and were classified as early (stage 1), mid (stage 3) and late (stage 4) LECs (Fig. 3A). The classification of eLECs, mLECs and ILECs was further supported by expression of stem/progenitor markers *HES4* and *ID3*, predominantly at early stages, whereas *PROX1* and *DACH2*, markers associated with lens development, were expressed during middle and late stages (Fig. 3C). GO enrichment

analysis highlighted significant biological processes at various differentiation stages, with ribosomes, oxidative respiratory chain, and ion transport being prevalent in early and middle stages. In contrast, markers associated with lens development and visual perception were highly expressed during the final stages of differentiation (Fig. 3D).

#### Age-related changes in human lens epithelium cell populations

After identifying subclasses of cells within the lens epithelium samples, the impact of aging was evaluated using UMAP to determine the distribution of cell type in aged and non-aged donors (Fig. 4A and B). The proportional distribution of cell types did not show significant differences between aged and non-aged groups (Fig. 4C and D). Interestingly, the Aged 3 sample with cataract

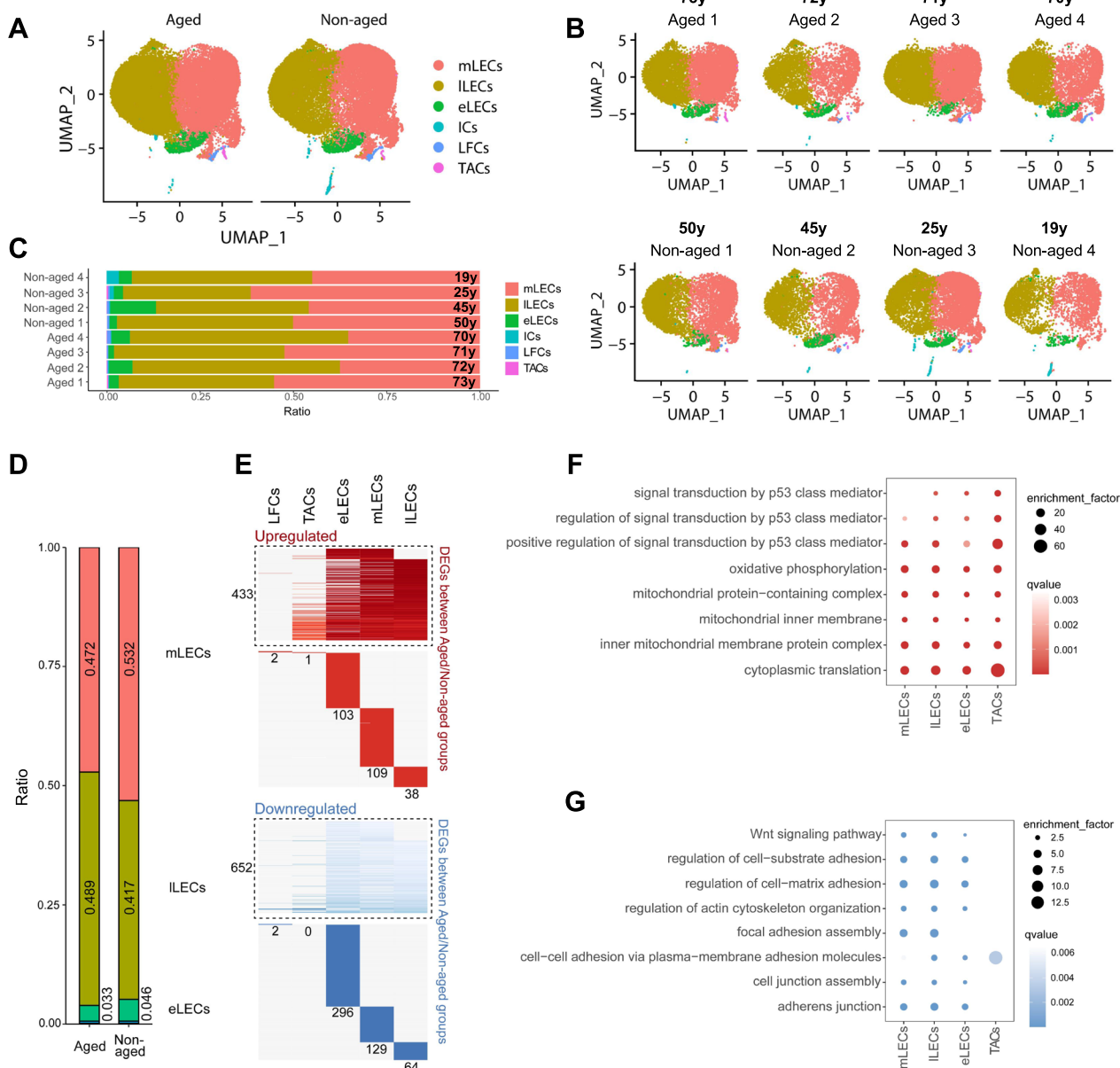


**Fig. 4** Changes in Different Cell Types between Aged and Non-aged Groups. **A** Integrated UMAP visualization of cell type composition in aged and non-aged groups. **B** Sample-specific UMAP projections demonstrating inter-individual variability. Colors represent cell types as in **A**. **C** Sample-specific stacked bar plot quantifying cellular composition. Bar width represents the proportion of this type of cell among all cells. **D** Integrated stacked bar plot of cell type composition in aged and non-aged groups. Numbers on bar indicate the proportion of cell types. **E** Heatmaps showing the distribution of upregulated (red) and downregulated (blue) DEGs for each cell type in human lens between the aged and non-aged groups. Genes not differentially expressed are in gray and the numbers of DEGs are indicated. The upper part (dotted lines) indicates the DEGs shared by at least 2 cell types, the lower panel indicated the unique DEGs of each cell type of each group. The numbers of gene are annotated on the plots. **F–G** Representative shared GO terms of **F** upregulated and **G** downregulated DEGs in different lens cell types. The color keys from white to red/blue indicate the range of q value (adjusted p value)

formation showed the lowest eLEC proportion among all aged groups (Fig. 4C), potentially suggesting an inverse correlation between eLEC abundance and cataract development. While cell distribution patterns appeared similar, at the transcriptomic level, significant numbers of

DEGs were detected in at least one cell type between aged and non-aged groups. This included 433 upregulated DEGs and 652 downregulated DEGs (Fig. 4E). Common processes associated with upregulated DEGs in the aged group, compared to the non-aged group,

included the regulation of mitochondrial and oxidative respiratory chain activities (Fig. 4F), whereas processes influenced by downregulated DEGs involved cytoskeletal organization and cell junctions (Fig. 4G). Overall, aging had minimal impact on the proportion of cells in the lens epithelium, but the transcriptome of these cells was sensitive to aging. Changes in gene expression profiles are likely to impact on physiologic functions.

### Identification and distribution of TACs

After clarifying the cell populations and age-related differences, we aimed to identify the mechanisms of homeostatic maintenance and damage repair in the lens in response to aging. Among the four LEC subpopulations, TACs exhibit the most well-defined transcriptomic profile, and their functional role is equally well characterized. TACs were notable for their low abundance but high expression of cell cycle-related genes, including *TOP2A*, *CENPF*, *BIRC5*, *MKI67*, *BUB1*, and *MAD2L1* (Fig. 5A and B). TACs from non-aged lenses were predominantly in the S phase for DNA synthesis (Fig. 5C), while TACs in aged lenses were more frequently in the G1 phase, indicating reduced proliferative activity. To further identify a reliable TAC marker, we analyzed transcriptome sequencing data from normal mouse lenses (Fig. 5D), which served as a crucial baseline for systematically excluding genes not expressed in normal lens tissue. The results demonstrated that all six candidate TAC markers were conserved across species, with *Top2a* exhibiting the highest expression level among them. The rate of cell division in the adult lens is relatively slow, and thus the number of TACs isolated and available for analysis is limited. To address this limitation, lens organoids derived from induced pluripotent stem cells were utilized (Fig. 5E). This approach captures different stages of lens growth and enables the observation of cell proliferation and fiber cell differentiation at varying levels of maturity. *TOP2A* expression peaked during the early to mid-stages and decreased with maturation, reaching its maximum earlier than *MAD2L1* and *BIRC5* (Fig. 5F). qRT-PCR validation revealed that *TOP2A* expression levels exhibited

a similar trend of change and were higher than those of other candidates (Fig. 5G). In summary, *TOP2A* was identified as a robust TAC marker in lens epithelium. *TOP2A*-positive staining was observed in the margins of mature organoids (Fig. 5H). Immunodetection of *TOP2A* provided definitive evidence for TAC populations in human lens epithelium. The expected location of TACs is the equator, which was confirmed by positive *TOP2A* staining in the equatorial epithelium of donor human lenses (Fig. 5I). In rabbit models of lens epithelial injury repair (Fig. 5J), *TOP2A*-positive cells were observed in the initial stage of lens regeneration (two weeks postoperatively). By 4 weeks post-operation, *TOP2A*-positive cells were rarely observed (Fig. 5K). This suggests that a considerable proportion of LECs may possess the potential to transform into TACs after lens injury, and subsequently return to a non-proliferative state as tissue repair and regeneration are accomplished.

### Identification and age-related differences in lens progenitor-like cells

Given that TACs arise from stem/progenitor cells through asymmetric division, we hypothesized that lens stem/progenitor cells are present in the upstream eLECs. eLECs were sub-clustered into two subpopulations: lens progenitor-like cells (LPLCs) and “other cells” (Fig. 6A). There was no significant difference in the proportion of LPLCs between aged and non-aged groups (Fig. S1A). Heatmap analysis revealed distinct gene expression profiles for the two cell types (Fig. 6B). DEGs highly expressed in LPLCs included *CCND1*, *HGF*, *HES5*, and *IDI* (Fig. 6C and D), which are known to maintain stemness in various organs [22–26]. Consistently, DEGs in LPLCs were enriched in cell proliferation and negative regulation of growth (Fig. 6E), suggesting that they exhibit a primitive, stem cell-like state. Comparison of LPLC gene expression between aged and non-aged groups revealed upregulated genes associated with apoptosis and senescence (Fig. 6F).

We further attempted to identify key genes regulating LPLC stemness. The baseline transcriptome data

(See figure on next page.)

**Fig. 5** Identification and Distribution of TACs in Lens. **A** Violin plots of expression level of 6 cell cycle-dependent genes that were selected for TAC characterization. **B** Spatial expression patterns of TAC candidate markers projected onto UMAP coordinates. Color gradient (gray → purple) reflects log-normalized counts. **C** Cell cycle phase distribution (G1/S/G2M) quantified in aged vs. non-aged groups. **D** Violin plots of the expression levels of the 6 TAC candidate markers from mouse lens transcriptome data. **E** ESC-derived lens organoid culture timeline (days 0–21). Brightfield inset shows typical morphology at key stages (scale bar, 1 mm). **F** The expression trends of the 6 TAC markers during organoid development by transcriptome sequencing. **G** qRT-PCR detection of TAC candidate markers during lens organoid development. **H** Immunofluorescence staining of *TOP2A*(+) cells in lens organoids during development (scale bar, 50 μm). **I** Distribution characteristics of *TOP2A*(+) cells in anterior and equatorial region of human lens epithelium (scale bar, 50 μm). **J** Schematic diagram of the rabbit lens regeneration model construction and the process of lens regeneration after surgery. **K** Immunofluorescence staining of *TOP2A*(+) cells on the rabbit lens sections at 2 and 4 weeks postoperatively (scale bar, 50 μm) Bars presented mean ± SD of 3 samples per group. \* $p < 0.05$ , \*\* $p < 0.01$ , and \*\*\* $p < 0.001$

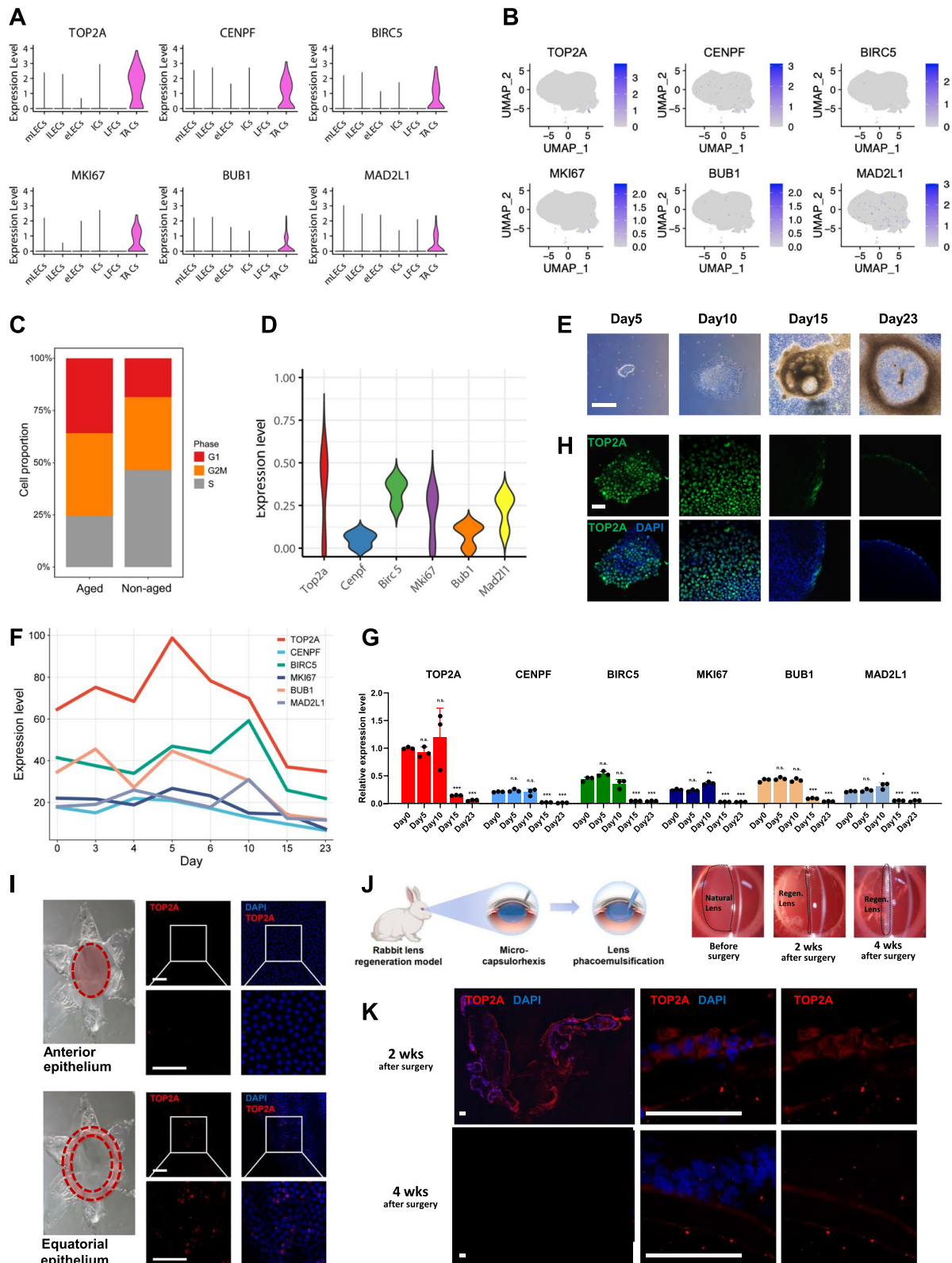


**Fig. 5** (See legend on previous page.)

from mouse lenses revealed that *Hgf* and *Hes5* were barely expressed in normal lens tissue, narrowing down the candidate genes to *CCND1* and *ID1* (Fig. 6G), with *ID1* expression peaking during the differentiation of lens organoids (Fig. 6H). qRT-PCR further confirmed the peak expression of *ID1* at day 10 and its sustained high expression level upon maturation (Fig. 6I). Cellular models of lens epithelial injury repair demonstrated *ID1* expression in HLECs at the leading edge of injury (Fig. 6J). In animal models of lens epithelial injury repair, *ID1*-positive cells were observed at the injured epithelial sites of regenerated rabbit lenses two weeks postoperatively, while the epithelium distal to the surgical wound showed nearly no *ID1*-positive cells (Fig. 6K), suggesting that activated lens stem/progenitor cells may facilitate repair via *ID1*-mediated mechanisms.

### Intercellular signaling networks regulating lens development and homeostasis

Understanding the interactions between different subpopulations within the lens epithelium is crucial. To investigate intercellular communication among LECs, CellChat DB analysis revealed extensive interactions between all four LEC populations, including TACs (Fig. 7A). However, interactions between LFCs and LECs were less pronounced. Significant secreted signaling pathways among the clusters are shown in Fig. 7B, with a focus on those involved in lens development and homeostasis (Fig. 7C). BMP signaling, which is crucial for lens placode formation [27, 28], primarily originated from eLECs and mainly targeted TACs. FGF signaling, predominantly originating from ILECs, plays a role in the differentiation of LECs into LFCs [27, 29]. WNT signaling, essential for LFC arrangement and lens placode development [27, 30], was mainly sourced from LFCs and eLECs.

In addition to the classical pathways of lens development, we identified a novel pleiotropic growth factor signaling network, namely pleiotrophin (PTN), which is strongly expressed (Fig. 6C). PTN signaling was widespread among all LEC populations, with higher expression of *Ptn* and its receptors *Sdc4*, *Sdc2*, and *Ncl* in the

mouse lens compared to components of the BMP/FGF/WNT pathways (Fig. 7D). Transcriptome sequencing of human lens organoids also revealed high expression of *PTN* and its ligands (Fig. 7E), suggesting that PTN networks may play a significant role in lens differentiation and homeostasis.

### Age-related changes in intercellular crosstalk in human lens epithelium

We compared intercellular networks between aged and non-aged groups to assess the effects of aging. Total intercellular interactions were reduced in the aged group, with significant alterations in BMP, FGF, PTN, and WNT signaling pathways (Fig. 8A). The number and intensity of interactions were notably lower in aged TACs, while some interactions received by eLECs were reduced in non-aged lenses, potentially as a compensatory mechanism (Fig. 8B).

To investigate the effects of aging on lens stem/progenitor cells, further analysis revealed a significant reduction in interactions between aged LPLCs and other cells, particularly with TACs (Fig. 8C). Among classic signaling pathways (Figs. 8D–F, S1B–E), we observed reduced signaling both emitted and received by LPLCs in the BMP network (Fig. 8D), accompanied by limited *BMPR2* expression (Fig. S1C). Changes in FGF and WNT signaling originating from ILECs were also observed (Fig. 8D). The impact of PTN signaling from aged LPLCs was markedly reduced, with the most pronounced decreases in *PTN-SDC2*, *PTN-SDC4*, and *PTN-NCL* signaling (Fig. 8E). *PTN* expression was also reduced in aged LPLCs (Fig. 8F). These findings suggest that PTN signaling not only regulates lens differentiation but also influences LPLC function and the maintenance of lens homeostasis.

### Discussion

In this study, we present a comprehensive analysis of the cellular composition of the human lens and age-related changes using scRNA-seq of lens superficial tissues from both non-aged and aged individuals. By mapping the transcriptomes of 56,717 cells from eight donors,

(See figure on next page.)

**Fig. 6** Identification and Age-Related Differences in Lens Progenitor-like Cells. **A** UMAP visualization of eLECs partitioned into two distinct subpopulations. **B** Heatmap showing the scaled expression levels of genes highly expressed specifically in the 2 subpopulations of eLECs. **C–D** Dedifferentiation signatures in LPLCs: **C** Dot plots and **D** feature plots showing the expression of dedifferentiation-related genes in LPLCs and other cells. **E** Top enriched GO terms for LPLCs compared with other cells. **F** Volcano plot of 327 DEGs in aged vs. non-aged LPLCs. **G** Mouse lens transcriptomes confirm LPLC marker (*Id1* and *Ccnd1*) conservation under normal condition. **H** The expression trends of dedifferentiation-related genes during organoid development by transcriptome sequencing. **I** qRT-PCR detection of *ID1*, *CCND1*, and *HGF* expression during lens organoid development. **J** Immunofluorescence staining of *ID1*(+) cells in the HLECs scratch healing assay (scale bar, 20  $\mu$ m). **K** Immunofluorescence staining of *ID1*(+) cells at wound margins on the rabbit capsule 2 weeks postoperatively (scale bar, 20  $\mu$ m). Bars presented mean  $\pm$  SD of 3 samples per group. \* $p < 0.05$ , \*\* $p < 0.01$ , and \*\*\* $p < 0.001$

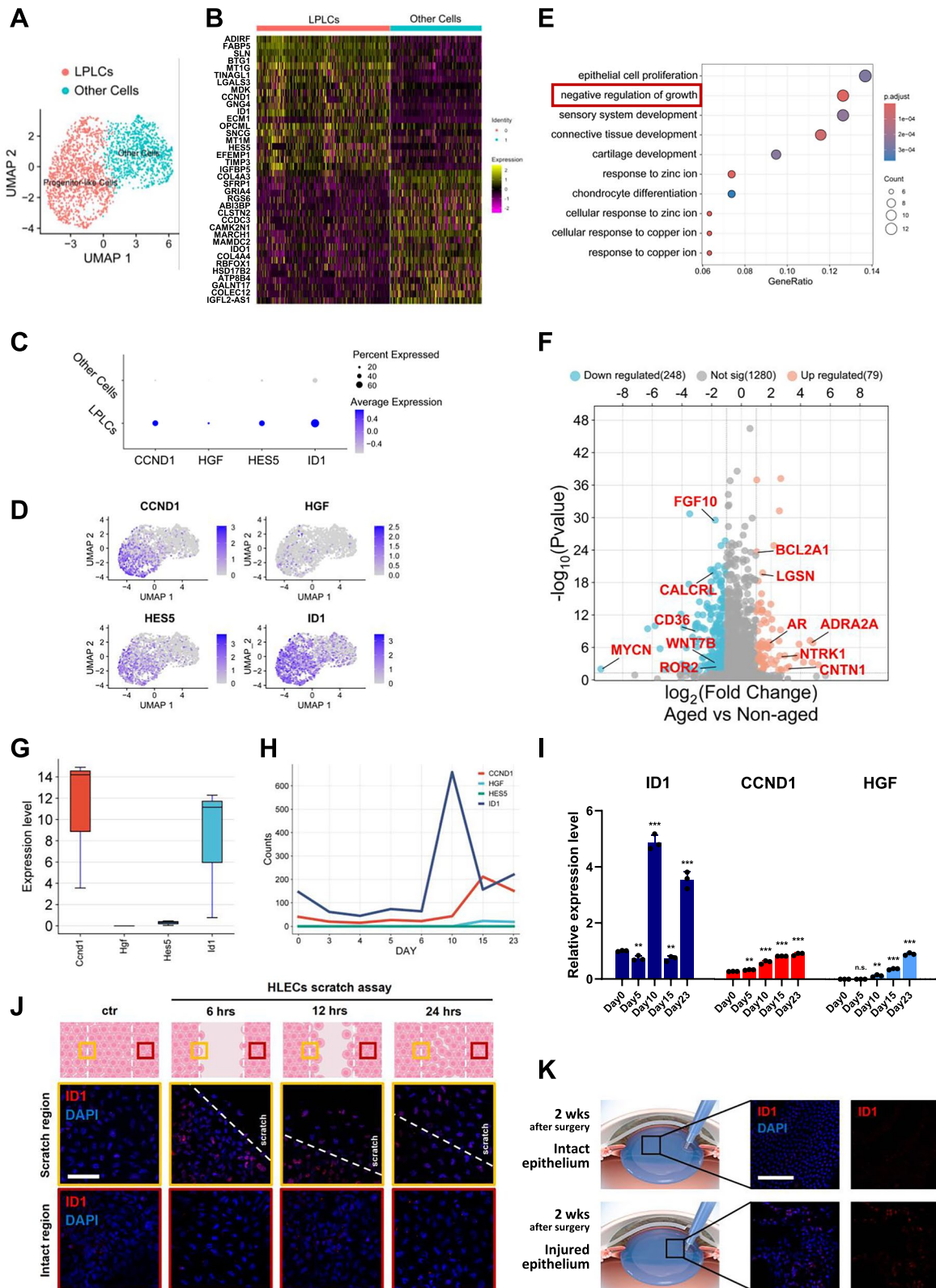


**Fig. 6** (See legend on previous page.)

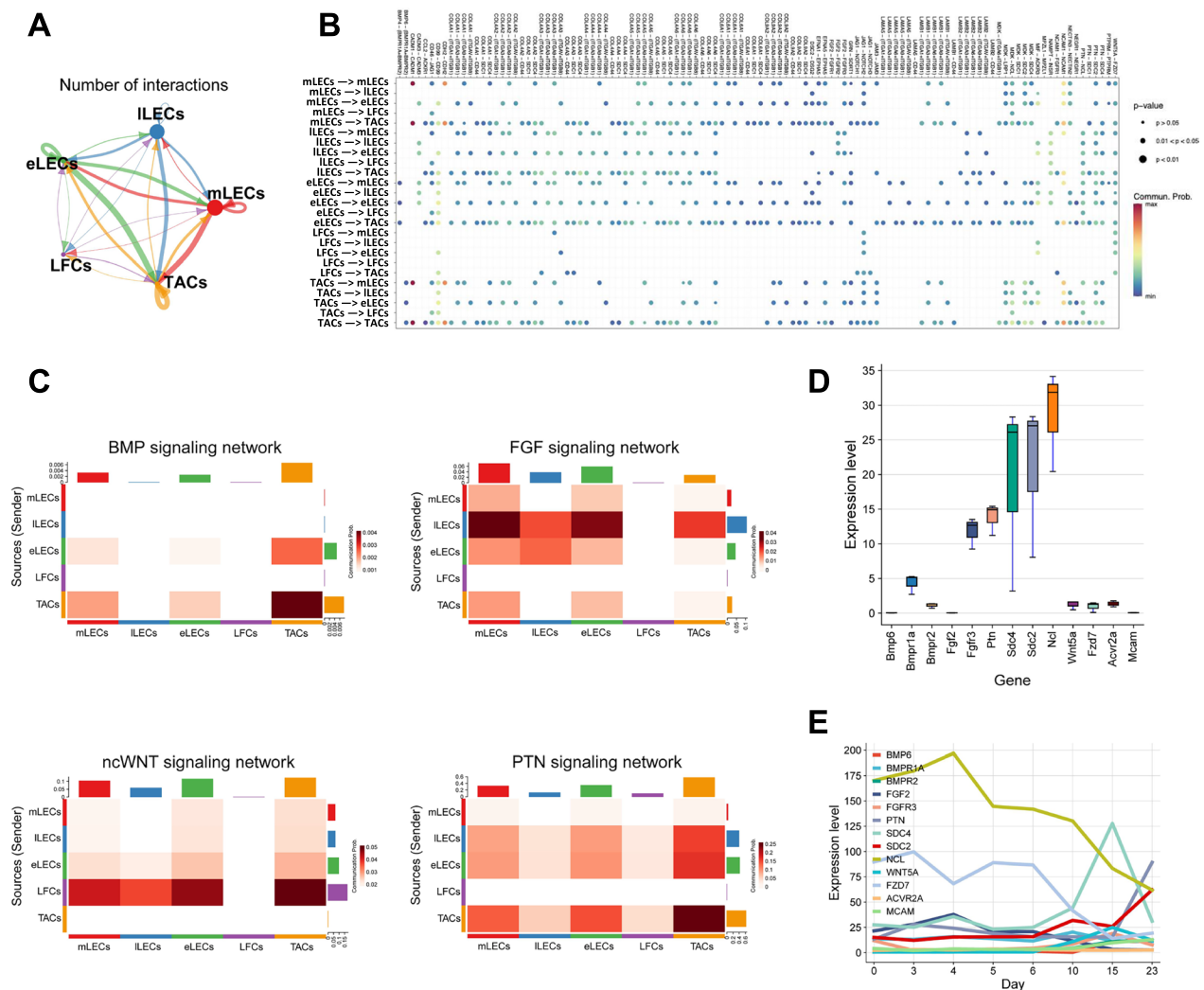


**Fig. 7** Intercellular Signaling Networks Regulating Lens Development and Homeostasis. **A** Global cell–cell communication landscape. Circle plot depicts interaction strength among 5 major clusters analyzed by CellChat DB. Edge thickness scales with communication probability. **B** Overview of the cellular networks regulating growth. Dot plot showing the inferred signaling networks among all cell populations. **C** Heatmap of BMP/FGF/WNT/PTN signaling networks in the cell–cell communication network. The top-colored bar plot indicates the sum of column values (incoming signaling), and the right bar plot indicates the sum of row values (outgoing signaling). The color key from white to red indicates low to high communication probability. **D** The expression levels of BMP/FGF/WNT/PTN-related genes from mouse lens transcriptome data. **E** The expression trends of BMP/FGF/WNT/PTN-related genes during organoid/development by transcriptome sequencing

(See figure on next page.)

**Fig. 8** Age-related changes in intercellular crosstalk in human lens epithelium. **A** Global communication changes. Vertical bar plots (upper) indicated the number and strength of interactions. Horizontal bar plot (lower) indicated the significant signaling pathways between aged and non-aged groups. The top signaling pathways colored red are more enriched in aged group; and the blue colored pathways are more enriched in non-aged group. **B** Differential interaction landscape. The top-colored bar plot indicates the sum of column values (incoming signaling), and the right bar plot indicates the sum of row values (outgoing signaling). Red indicates increased signaling in aged group compared to non-aged group, and blue indicates decreased signaling. **C** LPLC-specific communication. Chord diagram illustrates age-dependent polarity changes: Red color indicates that cellular interactions are stronger in the non-aged group and blue color indicates which are stronger in the aged group. **D** Comparative heatmap of BMP/FGF/WNT/PTN signaling networks. **E** Dot plot of the age-related ligand-receptor interaction of outgoing signaling from LPLCs. **F** Violin plots of PTN-related genes expression levels between aged and non-aged groups. **G** Schematic diagram of age-related changes in cell biological function in lens epithelium

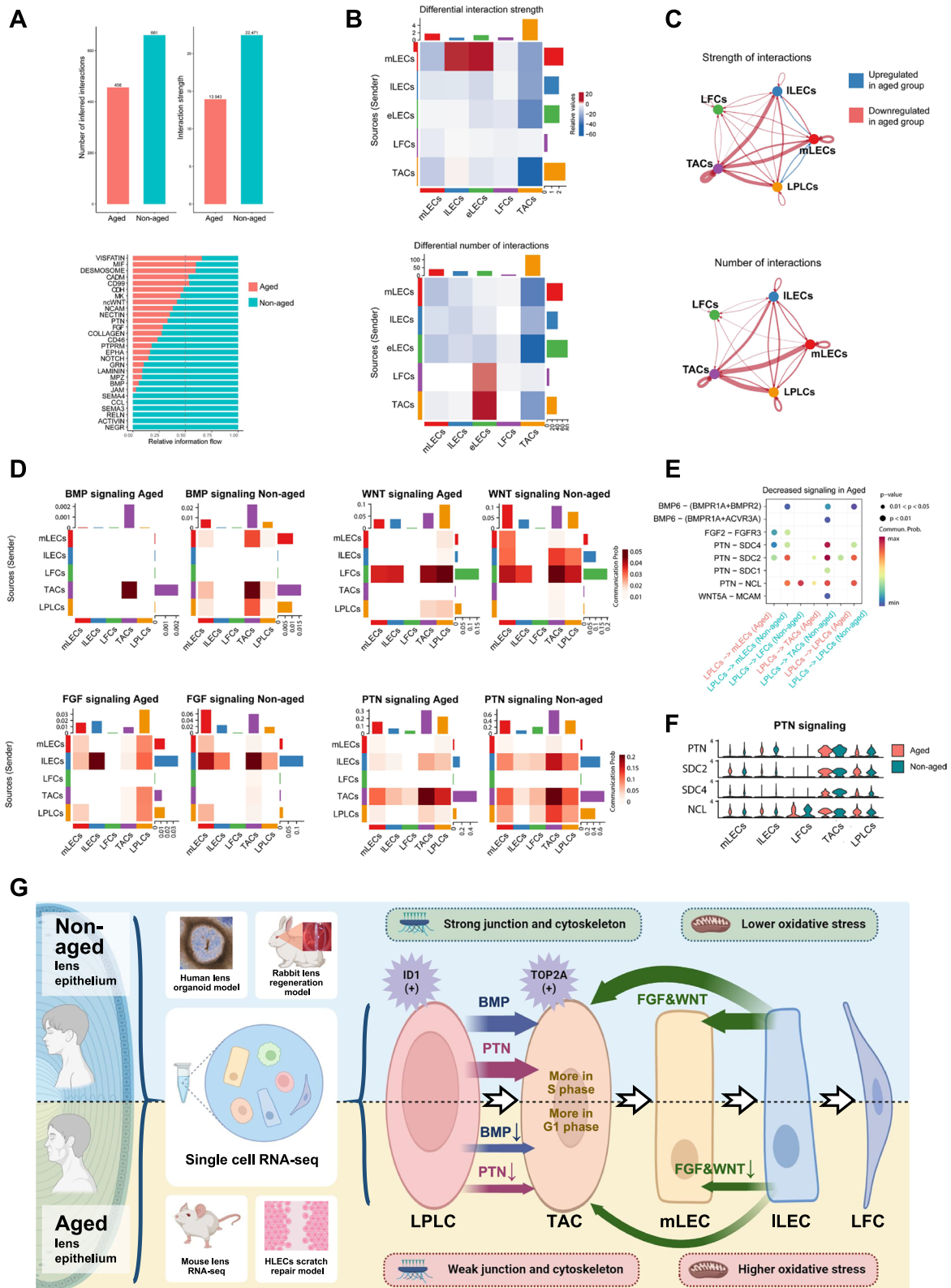


**Fig. 8** (See legend on previous page.)

we identified three major cell types within the samples, which, as expected, were predominantly LECs, a small population of residual LFCs, and ICs. The presence of ICs within the lens epithelium is noteworthy and supports previous reports indicating their presence in the lens [31, 32]. This cell population was not investigated in depth in the current study but certainly warrants more detailed analysis in future research. The primary focus of this study was the lens epithelial cell population.

In recent years, studies have been conducted to investigate the heterogeneity and subpopulations of human LECs, aiming to reveal their diverse manifestations across different regions and developmental stages [7, 33, 34]. Within this general classification, four LEC subclusters were identified based on gene expression profiles. Further analysis using CytoTRACE and RNA velocity outlined a putative differentiation pathway for LECs. eLECs, which are more primitive, differentiate into TACs, which undergo a limited period of rapid mitosis, produce new LECs, and subsequently differentiate into LFCs. The distinction between mLECs and lLECs lies in the fact that mLECs are closer to newly proliferated cells derived from TACs, whereas lLECs are best prepared to undergo fiber cell differentiation upon receiving the required signals. This finding helps delineate the progression of lens epithelial cells through developmental programs, which likely determine their function and fate. A recent scRNA-seq study identified two LEC subtypes based on *C8orf4* and *ADAMTSL4* expression [35], whereas our study offers a more detailed classification into four clusters and delineates a differentiation trajectory. The four populations were closely situated and partially interspersed in the UMAP plot (Fig. 2B), reflecting the underlying expression profile of the epithelial cell phenotype. However, signature patterns of relative expression enabled sub-classification and the establishment of four distinct groups.

In this study, we characterized the effect of aging on lens epithelial tissue for the first time using scRNA-seq. The demographic composition of the cell subpopulations did not change significantly with age, but distinct alterations were observed. We found that pathways downregulated in aged LECs were primarily associated with cell adhesion and junctions (Fig. 4G). Previous studies have shown that channel proteins in LECs, such as aquaporins (AQPs) and connexins (CXs), play critical roles in cell-cell and cell-matrix adhesion, which are essential for lens transparency [4, 36]. Aging progressively reduces AQPs and CXs, disrupting ion and fluid circulation and contributing to the development of ARCs [37]. A growing number of studies also indicate that dysfunction of focal adhesion kinase and integrin-linked kinase with aging mediates cataract formation [38]. We also found that the

common genes significantly upregulated in aged LECs were primarily associated with mitochondrial function and the oxidative respiratory chain (Fig. 4F). Mitochondrial dysfunction and the production of reactive oxygen species (ROS) have long been recognized as prominent mechanisms underlying cataract pathology [7, 39], which is consistent with our findings.

The existence of adult stem cells in the lens epithelium has been demonstrated through multiple lines of investigation. One research approach has focused on slow-cycling cell properties, utilizing conventional stem cell markers such as 3H-TdR or SOX2 to identify label-retaining cells in specific epithelial regions [11–14], potentially corresponding to LPLCs. Functional validation studies have further reinforced this concept, showing that single isolated lens epithelial cells can form clonal lens spheres capable of differentiating into lens organoids [40]. Notably, mammalian lens regeneration models following endocapsular extraction have revealed that residual PAX6+LECs can reconstitute complete lens structures [10], providing indirect but compelling evidence for LPLC populations. All the evidence reveals the existence of LPLCs, but their location remain a subject of debate. Many studies suggest that stem cells are located in the equatorial region of the human lens, within or near the germinative zone (GZ) [10, 13]. Other studies propose that stem cells reside in the central anterior epithelium, with equatorial cells representing limited proliferative cells [11, 12]. Our study demonstrated the presence of TACs in the equatorial region through TOP2A staining, but specific markers for lens stem cells have not yet been identified. We classified eLECs into LPLCs and “other cells”, both of which exhibit high differentiation potential. However, “other cells” are functional progenitor cells with a tendency to differentiate, whereas LPLCs maintain a more primitive, stem-like state. In LPLCs, ID1 may play a crucial role in maintaining their dedifferentiation properties. ID1, a transcriptional regulator, is typically expressed in both stem and progenitor cells and maintains self-renewal capacity by inhibiting differentiation [41–44]. ID1 has been found to be enriched in mouse basal epidermal progenitor cells, and its silencing impairs progenitor cell proliferation [41]. Moreover, lineage tracing of mouse intestinal epithelium revealed that ID1-positive cells are self-renewing pluripotent stem/progenitor cells and can serve as specific markers [42]. We observed high expression of ID1 in LEC injury repair models (Fig. 6I–K). These findings suggest that a subset of LECs may revert to primary progenitor cells with high differentiation potential, contributing to epithelial regeneration and healing. Overall, the understanding of lens adult stem cells requires further investigation.

Although the high proliferative potential of cells in the equatorial GZ has long been recognized, our study provides the first definitive identification of TACs in the lens. Here, we utilized the widely recognized cell-cycle-dependent genes from other tissues to characterize lens TACs. Among these markers, TOP2A can induce DNA double-stranded breaks, which catalyze DNA replication [45]. For example, in scRNA-seq of corneal limbus, the only cluster specifically expressing proliferation markers, including TOP2A, were identified as TACs [17, 46]. TOP2A plays a critical role in cell cycle regulation and is specifically highly expressed in rapidly proliferating cells [47]. By combining data from mouse lenses and lens organoids (Fig. 5D–G), we propose that TACs can be distinguished from other lens cells based on TOP2A expression. We observed a strikingly low abundance of TACs in the lens epithelium, significantly outnumbered by their upstream eLEC precursors. This quantitative disparity aligns precisely with the lens's unique tissue organization and homeostatic demands. Most LECs persist from birth with minimal turnover, resulting in very few proliferative TACs at any given time [48, 49]. But at the same time, a considerable LEC population retains a primitive, low-differentiation state throughout life [10]. Our identified eLECs likely represent these cells, which can be rapidly activated in the short term after injury (e.g., posterior capsule opacification after cataract surgery [50]; rabbit lens regeneration models in Fig. 5J–K, abundant TOP2A+ cells were detectable) to initiate disordered proliferation and regeneration.

Our findings reveal that classical signaling pathways involved in lens development, including FGF, BMP, and WNT, remain active among LEC populations (Fig. 7C). Additionally, we identify, for the first time, a potential role of PTN signaling in both lens differentiation and aging processes. PTN is a secreted cytokine that functions as a growth factor and plays a crucial role in the development of the nervous system and neuroplasticity [51]. PTN promotes the proliferation and differentiation of neural stem cells and contributes to maintaining the stability of the stem cell pool in the adult brain [52, 53]. The expression and activity of PTN decrease with age. Although both the nervous system and the lens originate from the ectoderm (the lens is derived from the surface ectoderm and the brain from the neuroectoderm), no study to date has reported the relevance of PTN to the lens. Our study reveals, for the first time, widespread PTN signaling among LEC types, with particularly high enrichment in TACs (Fig. 7C). In the nervous system, PTN receptors are diverse, and several studies have reported that neurotrophic activities are associated with its receptor SDC2 [54, 55]. This is consistent with our findings. In lens organoid, the expression trend of *SDC2*

closely parallels that of *PTN* compared to other receptors, with low levels early in development but steadily increasing towards the end (Fig. 7E). Therefore, the molecular mechanisms by which PTN regulates lens development and homeostasis require further investigation, especially downstream targets or interactions with canonical pathways like xFGF/BMP/WNT. Next, we will establish PTN gene-edited cell lines and animal models, combined with scRNA-seq data to conduct molecular biology studies, aiming to elucidate a novel signaling pathway regulating lens development and aging.

This study has several limitations. Although we identified TACs and LPLCs in human lens epithelial tissues, their precise spatial relationship—whether adjacent, staggered, or distant—remains unclear. To address this, we will perform spatial transcriptomics (10×Visium) on age-stratified human lens sections to map TAC/LPLC distributions at 55- $\mu\text{m}$  resolution, combined with multiplexed FISH to quantify intercellular distances between TACs and LPLCs. These data will be integrated with our scRNA-seq pseudotime trajectories to determine if differentiation follows a structured spatial pattern and whether age-related disorganization contributes to functional decline. Additionally, scRNA-seq captures only a small number of TACs and LPLCs, which limits the precision of the analysis. Given that TACs are predominantly distributed in the equatorial epithelium, we plan to perform scRNA-seq on the equatorial and anterior epithelium separately, enabling us to analyze the regional heterogeneity of LECs while increasing the proportion of TACs. Furthermore, the experimental validation of scRNA-seq results in animal models and organoid models is not sufficiently thorough or detailed, and further refinement is needed.

## Conclusions

Overall, this study elucidates the presence of LPLCs and TACs in the human lens, delineates a LPLC-TAC-dependent differentiation pathway during lens development, and demonstrates age-related changes in LECs, including alterations in cell adhesion and mitochondrial function. PTN signaling is implicated in both lens differentiation and the maintenance of stemness during aging. This research provides a comprehensive view of the single-cell transcriptional landscape and highlights cell-type-specific, aging-regulated signaling networks, advancing our understanding of age-related cataract pathogenesis.

## Abbreviations

LECs	Lens epithelial cells
LFCs	Lens fiber cells
ICs	Immune cells
TACs	Transient amplifying cells

eLECs	Early-differentiating lens epithelial cells
mLECs	Mid-differentiating lens epithelial cells
ILECs	Late-differentiating lens epithelial cells
LPLCs	Lens progenitor-like cells
scRNA-seq	Single-cell RNA sequencing
PTN	Pleiotrophin
ARCs	Age-related cataracts
3H-TdR	Tritiated thymidine
FBS	Fetal bovine serum
UMAP	Uniform manifold approximation and projection
GO	Gene ontology
DEGs	Differentially expressed genes
ESCs	Embryonic stem cells
DAPI	4,6-Diamido-2-phenylindole dihydrochloride
AQPs	Aquaporins
CXs	Connexins
ROS	Reactive oxygen species
GZ	Germinative zone
qRT-PCR	Quantitative real-time PCR

## Supplementary Information

The online version contains supplementary material available at <https://doi.org/10.1186/s13287-025-04436-w>.

Supplementary Material 1.

Supplementary Material 2.

Supplementary Material 3.

## Acknowledgements

We thank Jianyao Chen from the Eye Bank of the Second Affiliated Hospital of Zhejiang University for the assistance in obtaining donor samples. The work was supported by the National Natural Science Foundation of China (82471054, 82271063, 82201158, 8207939, 81870641, 81670833, 81300641), Key Research and Development Program of Zhejiang Province (2025C02157), Fundamental Research Funds of the Central Universities (2019QNA7026), and Central Guidance for Local Scientific and Technological Development Funding Program (2024ZY01057). The authors declare that they have not used AI-generated work in this manuscript.

## Author contributions

YG: Conceptualization, Methodology, Validation, Formal Analysis, Investigation, Writing—Original Draft, Visualization, LC: Conceptualization, Methodology, Software, Formal Analysis, Investigation, Writing—Original Draft, Visualization, SC: Validation, Formal Analysis, Investigation, YW: Validation, Formal Analysis, Investigation, SH: Conceptualization, Methodology, FS: Validation, Investigation, JY: Methodology, Investigation, ZQ: Project Administration, Methodology, DW: Conceptualization, YH: Project Administration, ZY: Validation, ZC: Writing—Review and Editing, IMW: Writing—Review and Editing, Supervision, YY: Conceptualization, Writing—Review and Editing, Project Administration, JQ: Methodology, Software, Formal Analysis, Writing—Review and Editing, QF: Conceptualization, Methodology, Writing—Review and Editing, Supervision, Project Administration, Funding Acquisition, KY: Conceptualization, Writing—Review and Editing, Supervision, Project Administration, Funding Acquisition.

## Funding

The work was supported by the National Natural Science Foundation of China (82471054, 82271063, 82201158, 8207939, 81870641, 81670833, 81300641), Key Research and Development Program of Zhejiang Province (2025C02157), Fundamental Research Funds of the Central Universities (2019QNA7026), and Central Guidance for Local Scientific and Technological Development Funding Program (2024ZY01057).

## Availability of data and materials

All data generated or analyzed during this study are included in this published article, its supplementary information files or GEO database under the accession number GSE287919 (<https://www.ncbi.nlm.nih.gov/geo/query/acc.cgi?acc=GSE287919>).

## Declarations

### Ethics approval and consent to participate

Ethical approval for this study was obtained from the Ethics Committee of the Second Affiliated Hospital of Zhejiang University. For the animal experiments, approval was granted for the project titled “Mechanisms of Age-Related Cataracts and Drug Screening” (Approval Number: 2024–0142; Date of approval: August 6, 2024). For the use of human-donated lenses, approval was obtained for the project titled “Study on Stemness Alterations and Differentiation Trajectories of Lens Epithelial Cells in Human-donated Lenses” (Approval Number: 2023–0641; Date of approval: June 23, 2023). The organ donor(s) or their guardian(s)/legally authorized representative(s) provided written informed consent for the use of samples. For ESCs, the original source (WiCell Research Institute, Inc.) has confirmed that there was initial ethical approval for collection of human cells, and that the donors had signed informed consent (<https://hpscereg.eu/cell-line/WAe009-A>). The Material Transfer Agreement has been included in the Supplementary Material 3. All procedures involving animals and human tissues were conducted in strict compliance with the approved ethical guidelines and regulations.

### Consent for publication

Not applicable.

### Competing interests

The authors declare that they have no competing interests.

### Author details

<sup>1</sup>Eye Center of the Second Affiliated Hospital, School of Medicine, Zhejiang Provincial Key Lab of Ophthalmology, Zhejiang Provincial Clinical Research Center for Eye Diseases, Zhejiang Provincial Engineering Institute on Eye Disease, Medical College of Zhejiang University, Hangzhou 310009, Zhejiang Province, China. <sup>2</sup>Human Eye Research Lab, Research Centre for Life Science and Healthcare, Nottingham Ningbo China Beacons of Excellence Research and Innovation Institute (CBI), University of Nottingham Ningbo China, Ningbo, Zhejiang Province, China. <sup>3</sup>Department of Environmental and Occupational Health, Zhejiang Provincial Center for Disease Control and Prevention, Hangzhou, Zhejiang Province, China. <sup>4</sup>Zhejiang Key Laboratory of Precision Diagnosis and Therapy for Major Gynecological Diseases, Women's Hospital, Zhejiang University School of Medicine, Hangzhou 310029, Zhejiang Province, China.

Received: 19 March 2025 Accepted: 9 June 2025

Published online: 01 July 2025

## References

- Asbell PA, Dualan I, Mindel J, Brocks D, Ahmad M, Epstein S. Age-related cataract. *Lancet* (London, England). 2005;365(9459):599–609. [https://doi.org/10.1016/s0140-6736\(05\)17911-2](https://doi.org/10.1016/s0140-6736(05)17911-2).
- Liu YC, Wilkins M, Kim T, Malyugin B, Mehta JS. Cataracts. *Lancet* (London, England). 2017;390(10094):600–12. [https://doi.org/10.1016/s0140-6736\(17\)30544-5](https://doi.org/10.1016/s0140-6736(17)30544-5).
- Chen X, Xu J, Chen X, Yao K. Cataract: advances in surgery and whether surgery remains the only treatment in future. *Adv Ophthalmol Pract Res*. 2021;1:100008. <https://doi.org/10.1016/j.aopr.2021.100008>.
- Liu Z, Huang S, Zheng Y, Zhou T, Hu L, Xiong L, et al. The lens epithelium as a major determinant in the development, maintenance, and regeneration of the crystalline lens. *Prog Retin Eye Res*. 2023;92: 101112. <https://doi.org/10.1016/j.preteyeres.2022.101112>.
- Duncan G, Wormstone IM, Davies PD. The aging human lens: structure, growth, and physiological behaviour. *Br J Ophthalmol*. 1997;81(10):818–23. <https://doi.org/10.1136/bjo.81.10.818>.
- Rakic JM, Galand A, Vrensen GF. Separation of fibres from the capsule enhances mitotic activity of human lens epithelium. *Exp Eye Res*. 1997;64(1):67–72. <https://doi.org/10.1006/exer.1996.0179>.
- Hawse JR, Hejtmančík JF, Horwitz J, Kantorow M. Identification and functional clustering of global gene expression differences between age-related cataract and clear human lenses and aged human lenses. *Exp Eye Res*. 2004;79(6):935–40. <https://doi.org/10.1016/j.exer.2004.04.007>.

8. Hawse JR, Hejtmancik JF, Huang Q, Sheets NL, Hosack DA, Lempicki RA, et al. Identification and functional clustering of global gene expression differences between human age-related cataract and clear lenses. *Mol Vis*. 2003;9:515–37.
9. Brunet A, Goodell MA, Rando TA. Ageing and rejuvenation of tissue stem cells and their niches. *Nat Rev Mol Cell Biol*. 2023;24(1):45–62. <https://doi.org/10.1038/s41580-022-00510-w>.
10. Lin H, Ouyang H, Zhu J, Huang S, Liu Z, Chen S, et al. Lens regeneration using endogenous stem cells with gain of visual function. *Nature*. 2016;531(7594):323–8. <https://doi.org/10.1038/nature17181>.
11. Saranya P, Shekhar M, Haripriya A, Muthukkaruppan V, Gowri PC. Towards the identification and characterization of putative adult human lens epithelial stem cells. *Cells*. 2023;12:23. <https://doi.org/10.3390/cells12232727>.
12. Zhou M, Leiberman J, Xu J, Lavker RM. A hierarchy of proliferative cells exists in mouse lens epithelium: implications for lens maintenance. *Invest Ophthalmol Vis Sci*. 2006;47(7):2997–3003. <https://doi.org/10.1167/iovs.06-0130>.
13. Yamamoto N, Majima K, Marunouchi T. A study of the proliferating activity in lens epithelium and the identification of tissue-type stem cells. *Med Mol Morphol*. 2008;41(2):83–91. <https://doi.org/10.1007/s00795-008-0395-x>.
14. Arnold K, Sarkar A, Yram MA, Polo JM, Bronson R, Sengupta S, et al. Sox2(+) adult stem and progenitor cells are important for tissue regeneration and survival of mice. *Cell Stem Cell*. 2011;9(4):317–29. <https://doi.org/10.1016/j.stem.2011.09.001>.
15. Camp JG, Wollny D, Treutlein B. Single-cell genomics to guide human stem cell and tissue engineering. *Nat Methods*. 2018;15(9):661–7. <https://doi.org/10.1038/s41592-018-0113-0>.
16. Wang D, Wang J, Bai L, Pan H, Feng H, Clevers H, et al. Long-term expansion of pancreatic islet organoids from resident procr(+) progenitors. *Cell*. 2020;180(6):1198–211.e19. <https://doi.org/10.1016/j.cell.2020.02.048>.
17. Li JM, Kim S, Zhang Y, Bian F, Hu J, Lu R, et al. Single-cell transcriptomics identifies a unique entity and signature markers of transit-amplifying cells in human corneal limbus. *Invest Ophthalmol Vis Sci*. 2021;62(9):36. <https://doi.org/10.1167/iovs.62.9.36>.
18. Fu Q, Qin Z, Jin X, Zhang L, Chen Z, He J, et al. Generation of functional lentoid bodies from human induced pluripotent stem cells derived from urinary cells. *Invest Ophthalmol Vis Sci*. 2017;58(1):517–27. <https://doi.org/10.1167/iovs.16-20504>.
19. Lyu D, Zhang L, Qin Z, Ni S, Li J, Lu B, et al. Modeling congenital cataract in vitro using patient-specific induced pluripotent stem cells. *NPJ Regen Med*. 2021;6(1):60. <https://doi.org/10.1038/s41536-021-00171-x>.
20. Qin Z, Zhang L, Lyu D, Li J, Tang Q, Yin H, et al. Opacification of lentoid bodies derived from human induced pluripotent stem cells is accelerated by hydrogen peroxide and involves protein aggregation. *J Cell Physiol*. 2019;234(12):23750–62. <https://doi.org/10.1002/jcp.28943>.
21. Chen X, Wang H, Chen H, Ren L, Wang W, Xu J, et al. Lens regeneration in situ using hESCs-derived cells -similar to natural lens. *iScience*. 2023;26(6):106921. <https://doi.org/10.1016/j.isci.2023.106921>.
22. Brett JO, Arjona M, Ikeda M, Quarta M, de Morrée A, Egner IM, et al. Exercise rejuvenates quiescent skeletal muscle stem cells in old mice through restoration of Cyclin D1. *Nat Metab*. 2020;2(4):307–17. <https://doi.org/10.1038/s42255-020-0190-0>.
23. Ding H, Wang Y, Zhang H. CCND1 silencing suppresses liver cancer stem cell differentiation and overcomes 5-fluorouracil resistance in hepatocellular carcinoma. *J Pharmacol Sci*. 2020;143(3):219–25. <https://doi.org/10.1016/j.jphs.2020.04.006>.
24. Fei MY, Wang Y, Chang BH, Xue K, Dong F, Huang D, et al. The non-cell-autonomous function of ID1 promotes AML progression via ANGPTL7 from the microenvironment. *Blood*. 2023;142(10):903–17. <https://doi.org/10.1182/blood.2022019537>.
25. Usunier B, Bossard C, L'Homme B, Linard C, Benderitter M, Milliat F, et al. HGF and TSG-6 released by mesenchymal stem cells attenuate colon radiation-induced fibrosis. *Int J Mol Sci*. 2021. <https://doi.org/10.3390/ijms22041790>.
26. Hitoshi S, Ishino Y, Kumar A, Jasmine S, Tanaka KF, Kondo T, et al. Mammalian Gcm genes induce Hes5 expression by active DNA demethylation and induce neural stem cells. *Nat Neurosci*. 2011;14(8):957–64. <https://doi.org/10.1038/nn.2875>.
27. Cvekl A, Zhang X. Signaling and gene regulatory networks in mammalian lens development. *Trends Genet TIG*. 2017;33(10):677–702. <https://doi.org/10.1016/j.tig.2017.08.001>.
28. Shu DY, Lovicu FJ. Insights into bone morphogenetic protein-(BMP-) signaling in ocular lens biology and pathology. *Cells*. 2021. <https://doi.org/10.3390/cells10102604>.
29. Robinson ML. An essential role for FGF receptor signaling in lens development. *Semin Cell Dev Biol*. 2006;17(6):726–40. <https://doi.org/10.1016/j.semcdb.2006.10.002>.
30. Shah R, Amador C, Chun ST, Ghiam S, Saghizadeh M, Kramerov AA, et al. Non-canonical Wnt signaling in the eye. *Prog Retin Eye Res*. 2023;95:101149. <https://doi.org/10.1016/j.preteyeres.2022.101149>.
31. Menko AS, DeDreu J, Logan CM, Paulson H, Levin AV, Walker JL. Resident immune cells of the avascular lens: mediators of the injury and fibrotic response of the lens. *FASEB J Off Publ Fed Am Soc Exp Biol*. 2021;35(4):e21341. <https://doi.org/10.1096/fj.202002200R>.
32. Walker JL, Menko AS. Immune cells in lens injury repair and fibrosis. *Exp Eye Res*. 2021;209:108664. <https://doi.org/10.1016/j.exer.2021.108664>.
33. Maidment JM, Duncan G, Tamiya S, Collison DJ, Wang L, Wormstone IM. Regional differences in tyrosine kinase receptor signaling components determine differential growth patterns in the human lens. *Invest Ophthalmol Vis Sci*. 2004;45(5):1427–35. <https://doi.org/10.1167/iovs.03-1187>.
34. Wormstone IM, Collison DJ, Hansom SP, Duncan G. A focus on the human lens in vitro. *Environ Toxicol Pharmacol*. 2006;21(2):215–21. <https://doi.org/10.1016/j.etap.2005.07.012>.
35. Zhu MC, Hu W, Lin L, Yang QW, Zhang L, Xu JL, et al. Single-cell RNA sequencing reveals new subtypes of lens superficial tissue in humans. *Cell Prolif*. 2023;56(1):e13477. <https://doi.org/10.1111/cpr.13477>.
36. Augusteyn RC. On the growth and internal structure of the human lens. *Exp Eye Res*. 2010;90(6):643–54. <https://doi.org/10.1016/j.exer.2010.01.013>.
37. Retamal MA, Altenberg GA. Role and posttranslational regulation of Cx46 hemichannels and gap junction channels in the eye lens. *Front Physiol*. 2022;13:864948. <https://doi.org/10.3389/fphys.2022.864948>.
38. Wederell ED, de longh RU. Extracellular matrix and integrin signaling in lens development and cataract. *Semin Cell Dev Biol*. 2006;17(6):759–76. <https://doi.org/10.1016/j.semcdb.2006.10.006>.
39. Lee B, Afshari NA, Shaw PX. Oxidative stress and antioxidants in cataract development. *Curr Opin Ophthalmol*. 2024;35(1):57–63. <https://doi.org/10.1097/icu.0000000000001009>.
40. O'Connor MD, McAvoy JW. In vitro generation of functional lens-like structures with relevance to age-related nuclear cataract. *Invest Ophthalmol Vis Sci*. 2007;48(3):1245–52. <https://doi.org/10.1167/iovs.06-0949>.
41. Kantzer CG, Yang W, Grommisch D, Vikhe Patil K, Mak KH, Shirokova V, et al. ID1 and CEBPA coordinate epidermal progenitor cell differentiation. *Development (Cambridge, England)*. 2022;149:22. <https://doi.org/10.1242/dev.201262>.
42. Zhang N, Yantiss RK, Nam HS, Chin Y, Zhou XK, Scherl EJ, et al. ID1 is a functional marker for intestinal stem and progenitor cells required for normal response to injury. *Stem Cell Rep*. 2014;3(5):716–24. <https://doi.org/10.1016/j.stemcr.2014.09.012>.
43. Shang S, Yang C, Chen F, Xiang RS, Zhang H, Dai SY, et al. ID1 expressing macrophages support cancer cell stemness and limit CD8(+) T cell infiltration in colorectal cancer. *Nat Commun*. 2023;14(1):7661. <https://doi.org/10.1038/s41467-023-43548-w>.
44. Singh SK, Singh S, Gadomski S, Sun L, Pfannenstien A, Magidson V, et al. Id1 ablation protects hematopoietic stem cells from stress-induced exhaustion and aging. *Cell Stem Cell*. 2018;23(2):252–65.e8. <https://doi.org/10.1016/j.stem.2018.06.001>.
45. Qin S, Yuan Y, Huang X, Tan Z, Hu X, Liu H, et al. Topoisomerase IIA in adult NSCs regulates SVZ neurogenesis by transcriptional activation of Usp37. *Nucleic Acids Res*. 2022;50(16):9319–38. <https://doi.org/10.1093/nar/gkac731>.
46. Quadri M, Baudouin C, Lotti R, Palazzo E, Campanini L, Bernard FX, et al. Characterization of skin interfollicular stem cells and early transit amplifying cells during the transition from infants to young children. *Int J Mol Sci*. 2024. <https://doi.org/10.3390/ijms25115635>.
47. Ben-David U, Cowell IG, Austin CA, Benvenisty N. Brief reports: controlling the survival of human pluripotent stem cells by small molecule-based targeting of topoisomerase II alpha. *Stem Cells (Dayton, Ohio)*. 2015;33(3):1013–9. <https://doi.org/10.1002/stem.1888>.

48. Colitz CM, Davidson MG, Mc GM. Telomerase activity in lens epithelial cells of normal and cataractous lenses. *Exp Eye Res.* 1999;69(6):641–9. <https://doi.org/10.1006/exer.1999.0739>.
49. Jarrin M, Pandit T, Gunhaga L. A balance of FGF and BMP signals regulates cell cycle exit and Equarin expression in lens cells. *Mol Biol Cell.* 2012;23(16):3266–74. <https://doi.org/10.1091/mbc.E12-01-0075>.
50. Lovicu FJ, Shin EH, McAvoy JW. Fibrosis in the lens. Sprouty regulation of TGF $\beta$ -signaling prevents lens EMT leading to cataract. *Exp Eye Res.* 2016;142:92–101. <https://doi.org/10.1016/j.exer.2015.02.004>.
51. Deuel TF, Zhang N, Yeh HJ, Silos-Santiago I, Wang ZY. Pleiotrophin: a cytokine with diverse functions and a novel signaling pathway. *Arch Biochem Biophys.* 2002;397(2):162–71. <https://doi.org/10.1006/abbi.2001.2705>.
52. Kadomatsu K, Muramatsu T. Midkine and pleiotrophin in neural development and cancer. *Cancer Lett.* 2004;204(2):127–43. [https://doi.org/10.1016/s0304-3835\(03\)00450-6](https://doi.org/10.1016/s0304-3835(03)00450-6).
53. Jung CG, Hida H, Nakahira K, Ikenaka K, Kim HJ, Nishino H. Pleiotrophin mRNA is highly expressed in neural stem (progenitor) cells of mouse ventral mesencephalon and the product promotes production of dopaminergic neurons from embryonic stem cell-derived nestin-positive cells. *FASEB J Off Publ Fed Am Soc Exp Biol.* 2004;18(11):1237–9. <https://doi.org/10.1096/fj.03-0927je>.
54. Landgraf P, Wahle P, Pape HC, Gundelfinger ED, Kreutz MR. The survival-promoting peptide Y-P30 enhances binding of pleiotrophin to syndecan-2 and -3 and supports its neuritogenic activity. *J Biol Chem.* 2008;283(36):25036–45. <https://doi.org/10.1074/jbc.M800963200>.
55. Neumann JR, Dash-Wagh S, Jack A, Räk A, Jüngling K, Hamad MK, et al. The primate-specific peptide Y-P30 regulates morphological maturation of neocortical dendritic spines. *PLoS ONE.* 2019;14(2):e0211151. <https://doi.org/10.1371/journal.pone.0211151>.

### Publisher's Note

Springer Nature remains neutral with regard to jurisdictional claims in published maps and institutional affiliations.